NASA Technical Memorandum 85720

NASA-TM-85720 19840003747

THE USE OF SINGULAR VALUE GRADIENTS AND OPTIMIZATION TECHNIQUES TO DESIGN ROBUST CONTROLLERS FOR MULTILOOP SYSTEMS

JERRY R. NEWSOM AND V. MUKHOPADHYAY

NOVEMBER 1983

National Aeronautics and Space Administration

Langley Research Center
Hampton, Virginia 23665

18 1 1 RN/NASA-TM-85720
DISPLAY 18/2/1
84N11815*# ISSUE 2 PAGE 277 CATEGORY 63 RPT#: NASA-TM-85720 NAS 1.15:85720 83/11/00 10 PAGES UNCLASSIFIED DOCUMENT
UTTL: The use of singular value gradients and optimization techniques to design robust controllers for multiloop systems
AUTH: A/NEWSOM, J. R.; B/MUKHOPADHYAY, V. PAA: B/(George Washington Univ., Washington, D.C.)
CORP: National Aeronautics and Space Administration. Langley Research Center, Hampton, Va. AVAIL.NTIS SAP: HC A02/MF A01
Presented at the AIAA Guidance and Control Conf., Gatlinburg, Tenn., 15-17 Aug. 1983
MAJS: /*CASCADE CONTROL/*CONTROLLERS/*GRADIENTS/*OPTIMIZATION
MINS: / FLIGHT CONTROL/ NUMERICAL ANALYSIS/ ROBUSTNESS (MATHEMATICS)
ABA: Author
ABS: A method for designing robust feedback controllers for multiloop systems is presented. Robustness is characterized in terms of the minimum singular value of the system return difference matrix at the plant input. Analytical gradients of the singular values with respect to design variables in the controller are derived. A cumulative measure of the singular values and their gradients with respect to the design variables is used with a numerical optimization technique to increase the system's robustness. Both unconstrained and constrained optimization techniques are evaluated. Numerical results are presented for a two output drone flight
ENTER:

THE USE OF SINGULAR VALUE GRADIENTS AND OPTIMIZATION TECHNIQUES TO DESIGN ROBUST CONTROLLERS FOR MULTILOOP SYSTEMS

Jerry R. Newsom*
NASA Langley Research Center
Hampton, Virginia

V. Mukhopadhyay†
George Washington University
Joint Institute for Advancement of Flight Sciences
Hampton, Virginia

Abstract

A method for designing robust feedback controllers for multiloop systems is presented. Robustness is characterized in terms of the minimum singular value of the system return difference matrix at the plant input. Analytical gradients of the singular values with respect to design variables in the controller are derived. A cumulative measure of the singular values and their gradients with respect to the design variables is used with a numerical optimization technique to increase the system's robustness. Both unconstrained and constrained optimization techniques are evaluated. Numerical results are presented for a two-input/two-output drone flight control system.

Nomenclature

A,B,C,D	controller matrices
$\bar{A},\bar{B},\bar{C}$	augmented system matrices
dB	decibel
F,G_u,H	plant matrices
G	plant transfer matrix
g	cumulative constraint
I	identity matrix
$[I+KG]$	return difference matrix
J	objective function
j	$\sqrt{-1}$
K	controller transfer matrix
k_n	nth loop gain in L matrix
L	diagonal gain and phase change matrix
M	order of controller
N_S,N_C,N_O	order of plant, input, and output
p	element of controller quadruple
r	reference input
s	Laplace variable
u	plant input vector
u_n,v_n	left and right eigenvectors
x	plant state vector
x_c	controller state vector
z	plant output vector
β	sideslip angle (deg)
δ_1,δ_2	elevon and rudder deflections (deg)
σ_n	nth singular value
$\bar{\sigma},\underline{\sigma}$	maximum and minimum singular value
$\underline{\sigma}_M,\underline{\sigma}_D$	global minimum and desired singular value
ϕ_n	nth loop phase in L matrix
$\phi,\dot{\phi}$	roll angle and rate (deg/sec)
$\psi,\dot{\psi}$	yaw angle and rate (deg/sec)
ω	frequency (rad/sec)
$[\ ]^*$	complex conjugate transpose of $[\ ]$
$(\dot{})$	represents time derivative of $(\ )$
$\mathrm{tr}[\ ]$	trace of a square matrix $[\ ]$

Introduction

A well-designed feedback control system should provide stability robustness with respect to plant uncertainty. For single-input/single-output systems, the classical concepts of gain and phase margins are employed as measures of system robustness. In multiloop systems, these classical single-loop measures may not always provide a good measure of system robustness. Recently, matrix singular value properties of a multiloop system's return difference matrix have been proposed as a measure of system robustness (1-4). Several authors have even related the singular values of the return difference matrix to multiloop gain and phase margins (3-4).

The majority of the effort to date has focused on singular values as analysis tools. Only a small amount of effort has been focused on the use of singular values for control law synthesis (5-7). Stein (5) discusses the frequency domain interpretation of the linear quadratic Gaussian (LQG) based design in terms of singular values. He shows how the LQG methodology can be used to design feedback controllers which satisfy design requirements expressed as singular value conditions. Safonov and Chen (7) discuss a procedure for maximizing singular values for stability margin optimization. The purpose of this paper is to introduce a new design method which employs a numerical optimization technique to search for the controller design variables that increase the minimum singular value of the system return difference matrix. The singular value

*Aerospace Engineer, Multidisciplinary Analysis and Optimization Branch, Loads and Aeroelasticity Division.
†George Washington University, Joint Institute for Advancement of Flight Sciences.

gradients required in the optimization schemes are derived analytically. Numerical results are computed for a two-input/two-output system which represents an experimental drone aircraft with a lateral attitude control system (8).

System Description

Let the multiloop feedback system shown in figure 1 be described by a set of constant coefficient differential equations of the form

Plant

$$\dot{x} = Fx + G_u u \tag{1}$$

$$z = Hx \tag{2}$$

Controller

$$\dot{x}_c = Ax_c + Bz \tag{3}$$

$$u = Cx_c + Dz \tag{4}$$

Equation (1) represents an N_s order plant having N_o output measurements, z, modeled by equation (2) and N_c control inputs, u. Equations (3) and (4) represent an Mth order feedback controller driven by the sensor output z. In terms of a transfer function matrix, the plant and the controller are

$$z = [H(Is-F)^{-1}G_u]u \equiv G(s)u \tag{5}$$

$$u = [C(Is-A)^{-1}B + D]z \equiv -K(s)z \tag{6}$$

respectively.

Assuming the closed-loop system to be stable, the robustness of the nominal system at the plant input can be examined by computing $\underline{\sigma}(I+KG)$ as a function of frequency ($s=j\omega$) and using the guaranteed stability criterion

$$\bar{\sigma}(L^{-1}-I) < \underline{\sigma}(I+KG) \tag{7}$$

at all frequencies (3). In this paper, the matrix L is a diagonal gain and phase change matrix at the input of the plant as shown in figure 1.

$$L = \text{Diag}\,[k_n e^{j\phi_n}]$$

The matrix L is the identity matrix for the nominal system and it can be shown that

$$\bar{\sigma}(L^{-1}-I) = \max_n \sqrt{(1-1/k_n)^2 + 2/k_n(1-\cos\phi_n)} \qquad n=1,2,\ldots N_c \tag{8}$$

Equation (8) is plotted in figure 2 with k_n and ϕ_n as parameters. This figure can be used to determine the gain margins for a particular phase margin for simultaneous changes of both gain and phase in all input channels (4).

Singular Value Gradient Derivation

In order to perform the optimization, it is necessary to determine the gradients of the singular value $\underline{\sigma}(I+KG)$ with respect to elements in the controller quadruple matrices A,B,C, and D. Let the parameter p represent one of the elements of the controller matrices which are the design variables. It was shown in reference 4 that for a distinct singular value σ_n of a complex matrix (I+KG), the gradient with respect to a real parameter p is given by

$$\frac{\partial \sigma_n(I+KG)}{\partial p} = \text{Re}\left[u_n^* \frac{\partial (I+KG)}{\partial p} v_n\right] \tag{9}$$

where v and u are respectively right and left normalized eigenvectors of (I+KG). (For repeated eigenvalues see reference 9 for the corresponding "Gateaux differential" expressions.)

It can be shown that

$$\frac{\partial \sigma_n(I+KG)}{\partial \hat{p}^T} = \text{Re}\left[\hat{H}(Is-\bar{A})^{-1}\bar{B}(v_n u_n^*)\right.$$

$$\left.[-I_i^! \bar{C}(Is-\bar{A})^{-1}\bar{T}]\right] \tag{10}$$

$$(N_o+M)x(N_c+M)$$

where

$$\hat{P} = \left[\begin{array}{c!c} D & C \\ \hline B & A \end{array}\right] \qquad \hat{H} = \left[\begin{array}{c!c} H & 0 \\ \hline 0 & I \end{array}\right]$$

$$(N_c+M)x(N_o+M) \qquad (N_o+M)x(N_s+M)$$

$$\bar{A} = \left[\begin{array}{c!c} F & 0 \\ \hline BH & A \end{array}\right] \qquad \bar{B} = \left[\begin{array}{c} G_u \\ \hline 0 \end{array}\right]$$

$$(N_s+M)x(N_s+M) \qquad (N_s+M)xN_c$$

$$\bar{C} = [-DH \,!\, -C] \qquad \bar{T} = \left[\begin{array}{c} 0 \\ \hline I \end{array}\right]$$

$$N_c x(N_s+M) \qquad (N_s+M)xM$$

To derive the matrix equation (10), define p as an element of the matrix P. Then the scalar equation (9) can be written as

$$\frac{\partial \sigma_n(I+KG)}{\partial p} = \mathrm{Re}\cdot \mathrm{tr}\, \frac{\partial (I+\bar{C}\Phi\bar{B})}{\partial p} v_n u_n^*$$

$$= \mathrm{Re}\cdot \mathrm{tr}[\{\partial\bar{C}/\partial p\Phi\bar{B}+\bar{C}\Phi\partial\bar{B}/\partial p+\bar{C}\Phi\partial\bar{A}/\partial p\Phi\bar{B}\}v_n u_n^*] \quad (11)$$

where $\Phi = (Is-\bar{A})^{-1}$. Note that

$$\partial\bar{B}/\partial p = 0$$

and

$$\bar{C} = \hat{I}_1\hat{P}\hat{H}$$
$$\bar{A} = \hat{F} + \hat{I}_2\hat{P}\hat{H} \quad (12)$$

where

$$\hat{I}_1 = [-I \,\vdots\, 0] \qquad \hat{I}_2 = \begin{bmatrix} 0 & \vdots & 0 \\ \cdots & & \cdots \\ 0 & \vdots & I \end{bmatrix}$$

$N_c \times (N_c+M)$ $\qquad$ $(N_s+M)\times(N_c+M)$

$$\hat{P} = \begin{bmatrix} F & \vdots & 0 \\ \cdots & & \cdots \\ 0 & \vdots & 0 \end{bmatrix}$$

$(N_s+M)\times(N_s+M)$

Equation (11) can be written as

$$\frac{\partial \sigma_n(I+KG)}{\partial p} = \mathrm{Re}\cdot \mathrm{tr}\left[\left\{\frac{\partial(\hat{I}_1\hat{P})}{\partial p} + \bar{C}\Phi\frac{\partial(\hat{I}_2\hat{P})}{\partial p}\right\}\hat{H}\Phi\bar{B}v_n u_n^*\right] \quad (13)$$

Using the matrix trace properties $\mathrm{Re}\ \mathrm{tr}(A)=\mathrm{Re}\ \mathrm{tr}(A^*)$, a matrix relation for the gradients with respect to all of the elements of $\hat{P}$ can be written as

$$\frac{\partial \sigma_n(I+KG)}{\partial \hat{P}} = \mathrm{Re}[\{\hat{I}_1^T+(\bar{C}\Phi\hat{I}_2)^*\}\{\hat{H}\Phi\bar{B}v_n u_n^*\}^*] \quad (14)$$

$(N_c+M)\times(N_o+M)$

The complex conjugate transpose of equation (14) gives equation (10). The gradient expressions for the matrices $(I+KG)^{-1}$, KG, $KG(I+KG)^{-1}$ can be obtained in the same manner and are given in the Appendix. Two additional computations are involved in computing singular value gradients at each frequency point. The first computation is the solution of a set of $(N_s + M)$ simultaneous equations and is relatively inexpensive since the matrix A is already available in upper Hessenberg form (10) from the computation of the singular values. The second is the computation of the eigenvectors and generally involves a low-order complex matrix.

Optimization Schemes

Let us assume that the minimum over the frequency domain of the singular value $\underline{\sigma}(I+KG)$ of a stable system is $\underline{\sigma}_M$. It is desired to increase $\underline{\sigma}_M$ to a desired value σ_D as illustrated in figure 3. An increased $\underline{\sigma}_M$ results in better gain and phase margins of the system as shown in equation (7) and figure 2. Optimization schemes to achieve this objective using the gradient information of equation (10) are described next.

Unconstrained Minimization Approach

In the unconstrained minimization approach, a single objective function J is minimized by changing the design variables p. Since $\underline{\sigma}(I+KG)$ is less than σ_D over a range of frequencies instead of at a single point, all of the violations where $\underline{\sigma}(I+KG) < \sigma_D$ are represented by a single cumulative measure J.

$$J(p) = \sum_i \left(\mathrm{Max}\{0,[\sigma_D-\underline{\sigma}(j\omega_i,p)]\}\right)^2 \quad (15)$$

The summation is taken over a large number of frequency points where both the choice of the frequency range and spacing of the frequency points in a frequency range are left to the designer. A geometric description of the cumulative objective function is shown in figure 3. The objective is to minimize (preferably reduce to zero) the shaded area below the σ_D line. A conjugate gradient algorithm (11) is used to search for the controller design variables p which minimize J without allowing $\underline{\sigma}$ to go near zero during the search process. Not allowing $\underline{\sigma}$ to go near zero is particularly important to avoid destabilizing the system during the linear search process, especially when $\underline{\sigma}$ has sharp drops at specific frequencies. The method is expected to work when $\underline{\sigma}$ and $\partial\underline{\sigma}/\partial p$ variations with frequency are not too large over small frequency ranges. If J can be reduced to zero, then the minimum singular value reaches σ_D or higher.

Constrained Minimization Approach

In the constrained minimization approach, an objective function J is minimized with respect to the design variables p subject to the inequality constraint $g \le 0$. In this approach the cumulative measure of all of the violations $\underline{\sigma}(I+KG) < \sigma_D$ is treated as the constraint (12). The objective function J and the constraint g are defined as

$$J(p) = 1/2\ \mathrm{tr}[C^T C] \tag{16}$$

$$g(p) = \sum_i \left(\mathrm{Max}\{0, [\underline{\sigma}_D - \underline{\sigma}(j\omega_i, p)]\}\right)^2 \tag{17}$$

The choice of J in equation (16) is desirable since a lower C is reflected in lower control activity. Other choices of J are possible. In equation (17), the summation is taken over a large number of frequency points as before. A geometric description of the cumulative constraint is shown in figure 3. The objective is to reduce the shaded area to zero by satisfying the inequality constraint $g \leq 0$. Although the present paper is confined to a single constraint, additional constraints on responses and singular value bounds at other points in the loop can be considered for an overall design. The method of feasible directions (11) is used to search for the controller design variables p which minimize J subject to $g \leq 0$. The method uses the objective function and constraint gradient information to determine a parameter move direction and a scalar multiplier in the usable-feasible direction to satisfy all constraints. When the constraint condition is satisfied, then $g \leq 0$ which implies $\underline{\sigma} > \sigma_D$ for all ω_i from the definition of g in equation (17).

Numerical Results

Numerical results are presented for a two-input/two-output system which represents a drone aircraft with a lateral attitude control system (4 and 8). A nominal controller is available for comparison. The present method is used to increase the robustness by redesigning the nominal controller. A block diagram of the drone lateral attitude control system is shown in figure 4 (8). The plant state vector x is defined as

$$x = \left[\beta\ \dot{\phi}\ \dot{\psi}\ \phi\ \delta_1/20\ \delta_2/20\right]^T$$

The plant matrices F, G_u, and H as defined in equations (1) and (2) are given in table 1. The nominal controller matrices A,B,C, and D as defined in equations (3) and (4) are given in table 2. The eigenvalues of the nominal open-loop and closed-loop system are given in table 3. The eigenvalue at $\lambda = 0.1889 \pm j1.051$ results in an unstable dutch roll mode. The elements of the input vector are the elevon and rudder actuator commands, respectively. All gain and phase changes are considered at the points X in figure 4. The minimum singular value of the return difference matrix (I+KG) over the operating frequency range is plotted in figure 5 for the nominal system. The minimum singular value is constant at 0.35 over low frequencies, then drops to its lowest value of 0.25 near 1.2 radians/sec which is close to the frequency of the unstable open-loop pole. The minimum singular value approaches unity asymptotically as KG attenuates at higher frequencies. Using the stability condition given in equation (7), the stability is guaranteed if $\bar{\sigma}(L^{-1}-I) < 0.25$. This can be interpreted in terms of gain and phase margins using figure 2. The guaranteed simultaneous gain margins are -2.0 dB and 2.5 dB ($\phi_1 = \phi_2 = 0$). The simultaneous phase margins are $\pm 15^0$ ($k_1 = k_2 = 0$ dB).

Figures 6a and 6b show the gradients of $\underline{\sigma}(I+KG)$ with respect to the nominal controller parameters a_{11}, a_{22},...d_{22}. The location of these parameters in the block diagram is shown in figure 4. The elements b_{11} and b_{22} do not show up in figure 4 since their unity values are embedded in the controller structure. The gradients with respect to c_{11} and d_{11} are quite large. The gradients with respect to other diagonal elements a_{11}, a_{22}, c_{22}, d_{22}, etc. are relatively small. These gradients attenuate to zero before 10 rad/sec except for the one with respect to d_{11} which attenuates at 30 rad/sec. It may be noted that although the off-diagonal elements are zero, the singular value gradients with respect to them are quite large.

Results of unconstrained minimization (Design 1). Unconstrained minimization is performed using c_{11} and d_{22} as the design parameters. The desired minimum singular value σ_D is 0.6. The equality relations $d_{11} = 0$ and $c_{22} = a_{22}$. d_{22} are maintained to satisfy the 1/s and s/(s+2) structure of the nominal control law. Hence the design parameters are basically proportional to gains in each loop. Although the convergence pattern of both the objective function and the design variables are not shown, the objective function reduces to zero in one iteration and the values of c_{22} and d_{22} are 0.13 and 9.69, respectively. Note that $c_{22} = -2d_{22} = -19.38$. The singular value plot is shown in figure 7 as design 1. The minimum singular value σ_M is 0.6 as desired. The price paid for the higher value of σ_M is the loss of rapid attenuation at higher frequencies. With $\sigma_M = 0.6$, the guaranteed gain margins are -4.1 dB and 8.0 dB and the phase margins are $\pm 35°$. This reflects substantial improvement over the nominal stability margins. The eigenvalues of the closed-loop system are given in table 3.

Results of constrained minimization (Design 2). Next the same problem is solved using the constrained optimization approach defined as design 2. The desired minimum singular value σ_D is again 0.6. The objective function is chosen as defined by equation (16). The convergence pattern for design 2 is shown in figure 8. The J and g are normalized by their starting value J_0 and g_0, respectively. The constraint is satisfied in three iterations but at the cost of increased J. The values of c_{11} and d_{22} after five iterations are 2.08×10^{-6} and 5.91, respectively. The corresponding singular value plot is shown in figure 7 as design 2. The minimum singular value $\sigma_M = 0.68$. The loss of attenuation at higher frequencies is much less as compared to design 1, probably because the algorithm tries to minimize the growth of $0.5(c_{11}^2 + c_{22}^2)$ as well. The eigenvalues of the closed-loop system are given in table 3.

As a general rule, an increase in robustness is accompanied by degraded response and increased control activity. This effect is examined from time response plots of the closed-loop system using the nominal, design 1, and design 2 controllers presented in figures 9a through 9e. The input is a unit ramp-hold elevon command which rises linearly from 0 to 1 in 0.4 seconds as shown in figure 9a. The sideslip β response is shown in figure 9b. The increase in sideslip from the nominal are roughly four times for design 1 and twice for design 2. Figures 9c and 9d show that the roll and yaw rates are 10 to 20% lower than nominal. The elevon activity increases by 25% for design 1 and 10% for design 2. The increase in rudder activity is roughly three times for design 1 and twice for design 2 with large initial overshoot.

Conclusions

A method for designing feedback controllers to increase the robustness of multiloop systems has been presented. Gradients of the singular values of the return difference matrix with respect to design variables in the controller were derived analytically. A cumulative measure of the singular values and their gradients was used with a numerical optimization algorithm to increase the system's robustness.

A numerical example was given to illustrate the method. For the example, a nominal controller was available. The present method was used to design a new controller which provided increased robustness. The global minimum singular value was increased substantially using both the unconstrained optimization approach and the constrained optimization approach. For both of these cases, the time response of the system using these controllers was degraded. Some high frequency attenuation was lost. For a better overall design, more constraints need to be added.

References

1. Safonov, M. G.; Laub, A. J.; and Hartmann, G. L.: Feedback Properties of Multivariable Systems: The Role and Use of the Return Difference Matrix. IEEE Trans. Auto. Control, Vol. AC-26, No. 1, Feb. 1981, pp. 47-65.

2. Doyle, J. C.; and Stein, G.: Multivariable Feedback Design: Concepts for a Classical/ Modern Synthesis. IEEE Trans. Auto. Control, Vol. AC-26, No. 1, Feb.1981, pp. 4-16.

3. Lehtomaki, N. A.; Sandell, N. S., Jr.; and Athans, M.: Robustness Results in Linear Quadratic Gaussian Based Multivariable Control Designs. IEEE Trans. Auto. Control, Vol. 26, No. 1, Feb. 1981, pp. 75-92.

4. Mukhopadhyay, V.; and Newsom, J. R.: Application of Matrix Singular Value Margins of Multiloop Systems. NASA TM-84524, July 1982.

5. Stein, G.: LQG-Based Multivariable Design: Frequency Domain Interpretation. AGARD Lecture Series 117, Multivariable Analysis and Design Techniques, Sept. 1981.

6. Doyle, J. C.: Multivariable Design Techniques Based on Singular Value Generalizations of Classical Control. AGARD Lecture Series 117, Multivariable Analysis and Design Techniques, Sept. 1981.

7. Safonov, M. G.; and Chen, B. S.: Multivariable Stability-Margin Optimisation With Decoupling and Output Regulation. IEE PROC, Vol. 129, Pt.D,No. 6, Nov. 1982, pp. 276-282.

8. Perry, B.: Methodology for Determining Elevon Deflections to Trim and Maneuver The DAST Vehicle with Negative Static Margin. NASA TM-84499, May 1982.

9. Freudenberg, J. S.; Looze, D. P.; and Cruz, J. B.: Robustness Analysis Using Singular Value Sensitivities. Int. J. Control, Vol. 35, No. 1, 1982, pp. 95-116.

10. Laub, A. J.: Efficient Multivariable Frequency Response Computations. IEEE Trans. Auto. Control, Vol. AC-26, No. 2, April 1981, pp. 407-408.

11. Vanderplaats, G. N.: CONMIN-A FORTRAN Program for Constrained Function Minimization-User Manual. NASA TM X-62282, Aug. 1973.

12. Greene, W. H.; and Sobieszczanski-Sobieski, J.: Minimum Mass Sizing of a Large Low-Aspect Ratio Airframe for Flutter-Free Performance. J. of Aircraft, Vol. 19, No. 3, March 1982, pp. 228-234.

Appendix

The singular value gradients of some useful matrices with respect to the controller quadruple $\hat{P}$ is presented in this appendix. The left and right eigenvectors u_n and v_n in each expression belong to the singular value of that particular matrix.

$$\frac{\partial \sigma_n (I+KG)^{-1}}{\partial \hat{P}^T} = -\mathrm{Re}\left[\hat{H}_\Phi a \overline{B} v_n u_n^* \left[-(I+KG)^{-1} \right]_i^i \overline{C}_\Phi a^T \right] \right] \qquad (A.1)$$

$$\frac{\partial \sigma_n (KG)}{\partial \hat{P}^T} = \mathrm{Re}\left[\hat{H}_\Phi \overline{B} v_n u_n^* \left[-I_i^i \overline{C}_\Phi T \right] \right] \qquad (A.2)$$

$$\frac{\partial \sigma_n(KG(I+KG)^{-1}}{\partial \bar{p}^T} = \mathrm{Re}[\hat{H}\Phi_a \bar{B} v_n u_n^* [-(I+KG)^{-1}] \quad (A.3)$$

$$\bar{C}\Phi_a \bar{\Gamma}]]$$

where $\Phi_a = (I_s - \bar{A} + \bar{B}\bar{C})^{-1}$ (A.4)

The gradient expression for $\sigma(GK)$ etc. at the output can be derived similarly starting from equation 9.

Table 1 Plant matrices F, G_u, and H for drone lateral attitude control system

$$F = \begin{bmatrix} -.08527 & -0.0001423 & -0.9994 & 0.04142 & 0 & 0.1862 \\ -46.86 & -2.757 & 0.3896 & 0 & -124.3 & 128.6 \\ -0.4248 & -0.06224 & -0.06714 & 0 & -8.792 & -20.46 \\ 0 & 1 & 0 & 0 & 0 & 0 \\ 0 & 0 & 0 & 0 & -20.0 & 0 \\ 0 & 0 & 0 & 0 & 0 & -20.0 \end{bmatrix}$$

$$G_u = \begin{bmatrix} 0 & 0 \\ 0 & 0 \\ 0 & 0 \\ 0 & 0 \\ 1 & 0 \\ 0 & 1 \end{bmatrix} \qquad H = \begin{bmatrix} 0 & 1 & 0 & 0 & 0 & 0 \\ 0 & 0.07 & 1 & 0 & 0 & 0 \end{bmatrix}$$

Table 2 Controller quadruple matrices A, B, C, and D for drone lateral attitude control system

$$A = \begin{bmatrix} 0 & 0 \\ 0 & -2 \end{bmatrix} \qquad B = \begin{bmatrix} 1 & 0 \\ 0 & 1 \end{bmatrix}$$

$$C = \begin{bmatrix} 1.0 & 0 \\ 0 & -4.116 \end{bmatrix} \qquad D = \begin{bmatrix} 0 & 0 \\ 0 & 2.058 \end{bmatrix}$$

Table 3 Eigenvalues of drone lateral attitude control system

MODE	OPEN LOOP	CLOSED LOOP		
		NOMINAL	DESIGN-1	DESIGN-2
1	-0.03701	-0.6911	-0.0386	-0.01399
2, 3	0.1889 ± j 1.051	-0.2553 ± j 1.187	-0.6436 ± j 0.823	-0.5336 ± j 0.959
4	-3.25	-2.60	-6.225 ± j 2.342	-3.866 ± j 2.276
5	-20.0	-18.70	-11.11	-16.08
6	-20.0	-20.15	-20.02	-20.00
7		0	0	0
8		-2.261		

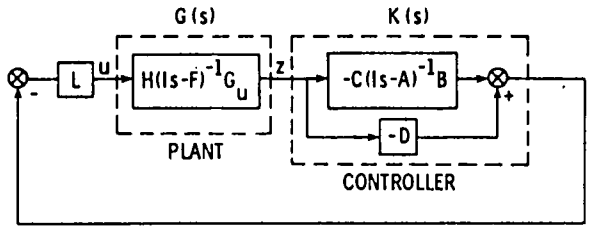

Fig. 1 Block diagram of a multiloop system.

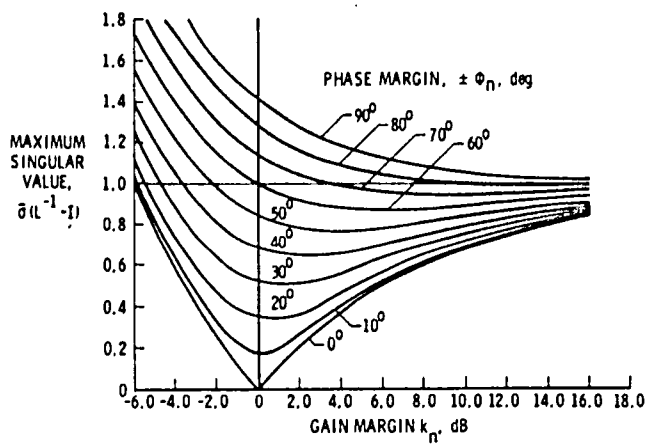

Fig. 2 Universal diagram for gain-phase margin evaluation.

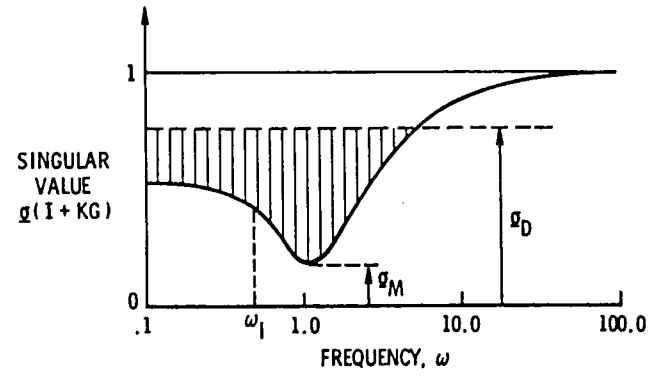

Fig. 3 Geometric description of cumulative objective function and cumulative constraints.

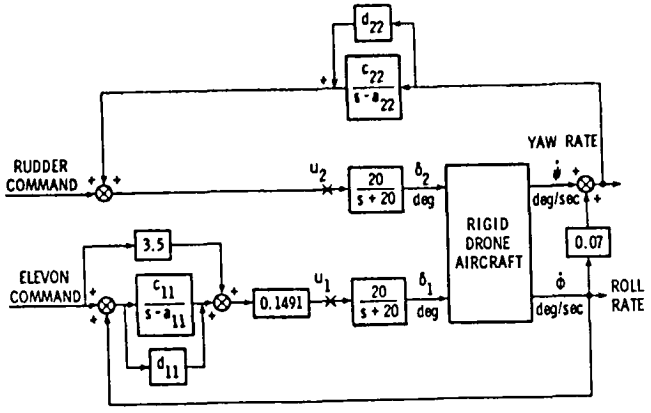

Fig. 4 Block diagram of a drone lateral attitude control system.

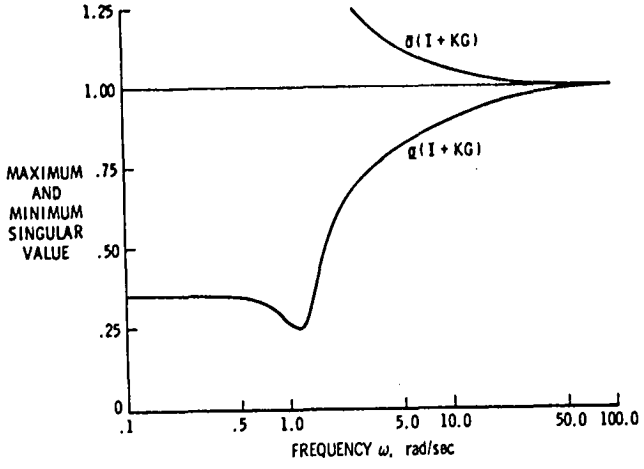

Fig. 5 Maximum and minimum singular value vs. frequency for drone attitude control system (nominal).

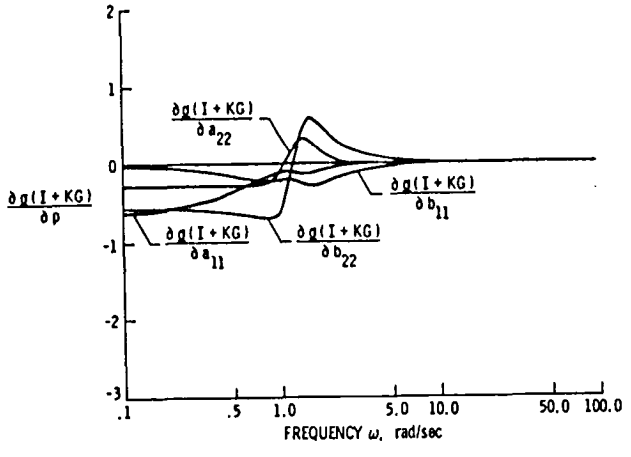

Fig. 6(a) Gradient of singular value $\underline{\sigma}(I+KG)$ with respect to controller parameters a_{11}, a_{22}, b_{11}, and b_{22} (nominal).

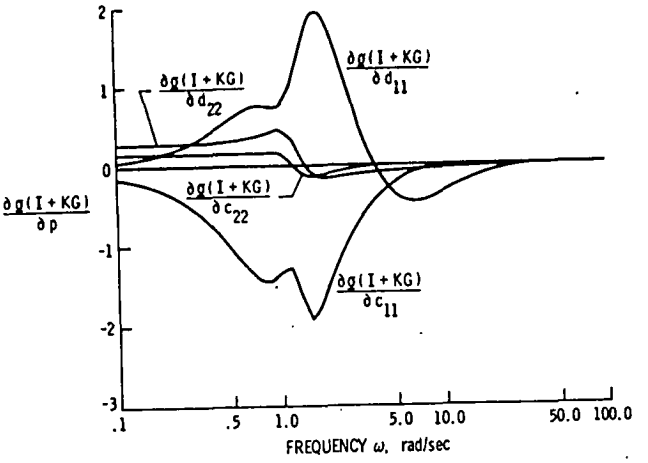

Fig. 6(b) Gradient of singular value $\underline{\sigma}(I+KG)$ with respect to controller parameters c_{11}, c_{22}, d_{11}, and d_{22} (nominal).

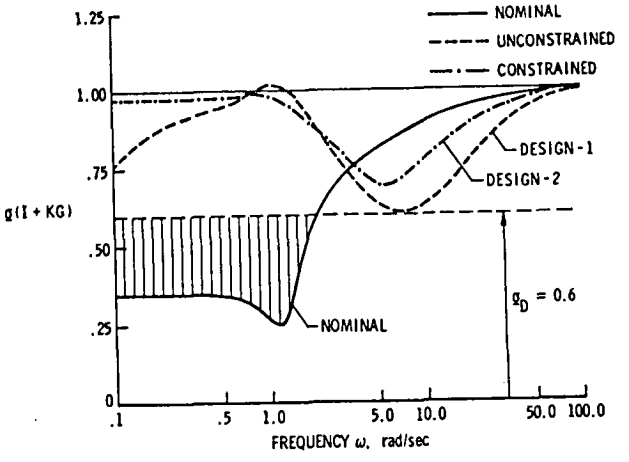

Fig. 7 Minimum singular value vs. frequency plot for nominal and optimized control laws.

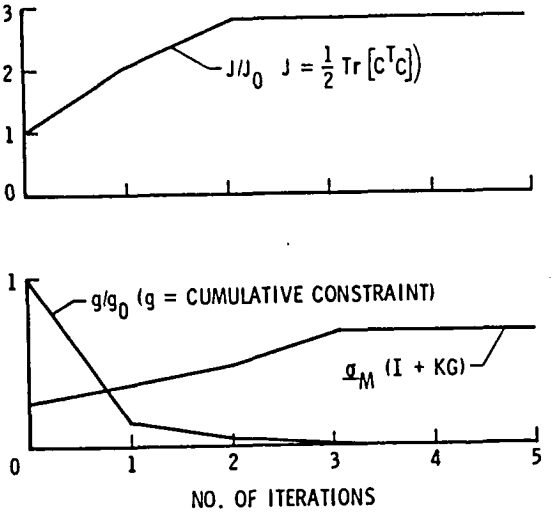

Fig. 8 Convergence pattern of constrained minimization (Design 2).

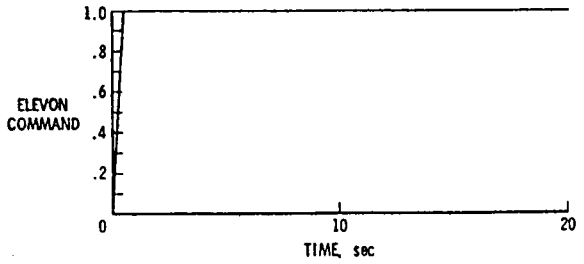

Fig. 9(a) Ramp-hold elevon command.

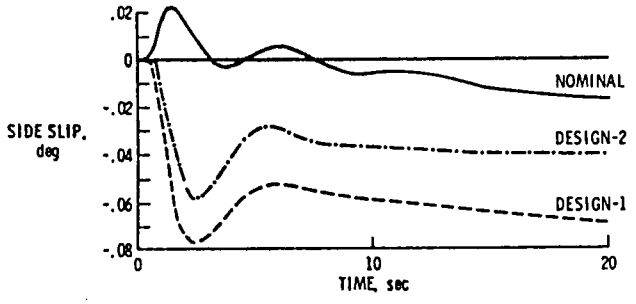

Fig. 9(b) Side slip response to ramp-hold elevon command.

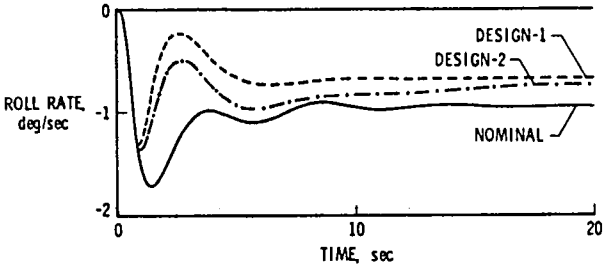

Fig. 9(c) Roll rate response to ramp-hold elevon command.

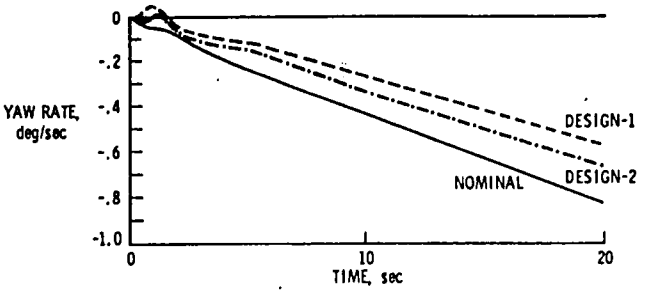

Fig. 9(d) Yaw rate response to ramp-hold elevon command.

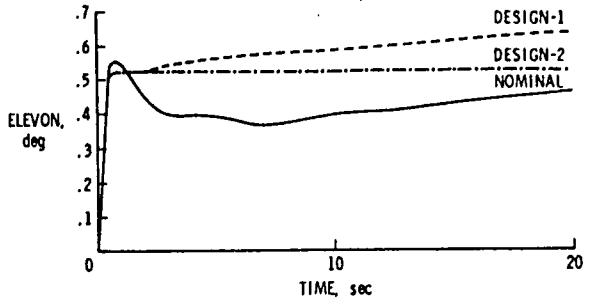

Fig. 9(e) Elevon deflection response to ramp-hold elevon command.

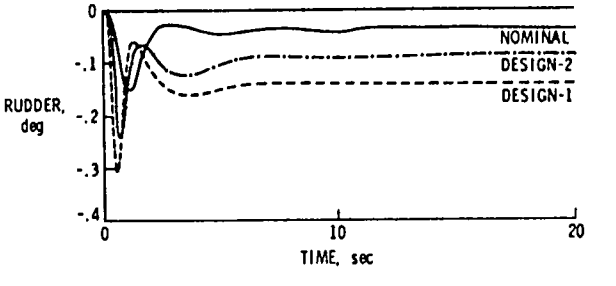

Fig. 9(f) Rudder deflection response to ramp-hold elevon command.

1. Report No.	2. Government Accession No.	3. Recipient's Catalog No.
NASA TM-85720		

4. Title and Subtitle	5. Report Date
The Use of Singular Value Gradients and Optimization Techniques to Design Robust Controllers for Multiloop Systems	November 1983
	6. Performing Organization Code 505-33-43-13
7. Author(s) Jerry R. Newsom* and V. Mukhopadhyay**	8. Performing Organization Report No.
	10. Work Unit No.
9. Performing Organization Name and Address NASA Langley Research Center Hampton, VA 23665	11. Contract or Grant No.
	13. Type of Report and Period Covered Technical Memorandum
12. Sponsoring Agency Name and Address National Aeronautics and Space Administration Washington, DC 20546	14. Sponsoring Agency Code

15. Supplementary Notes *NASA Langley Research Center, **George Washington University
Presented at the AIAA Guidance and Control Conference
August 15-17, 1983
Gatlinburg, Tennessee AIAA Paper 83-2191CP

16. Abstract

A method for designing robust feedback controllers for multiloop systems is presented. Robustness is characterized in terms of the minimum singular value of the system return difference matrix at the plant input. Analytical gradients of the singular values with respect to design variables in the controller are derived. A cumulative measure of the singular values and their gradients with respect to the design variables is used with a numerical optimization technique to increase the system's robustness. Both unconstrained and constrained optimization techniques are evaluated. Numerical results are presented for a two-input/two-output drone flight control system.

17. Key Words (Suggested by Author(s))	18. Distribution Statement
Multiloop systems Robustness Numerical optimization technique	Unclassified - Unlimited Star Category - 63

19. Security Classif. (of this report)	20. Security Classif. (of this page)	21. No. of Pages	22. Price
Unclassified	Unclassified	9	A02